IMPACT RECOVERY OF SELF-HEALING COMPOSITES BASED ON A SUPRAMOLECULAR POLYMER MATRIX

Federica Sordo, Lucien Berret, Baris Caglar and Véronique Michaud

Laboratory for Processing of Advanced Composites (LPAC), Institute of Materials, Ecole Polytechnique Fédérale de Lausanne (EPFL), CH-1015 Lausanne, Switzerland
veronique.michaud@epfl.ch
lpac.epfl.ch

Keywords: Fibre Reinforced Composites (FRC), intrinsic self-healing, supramolecular polymers, impact test

ABSTRACT

We investigated the extent of damage and ability to heal cracks after low velocity impact of glass fibre reinforced composites (FRCs) with a matrix based on a supramolecular hybrid network, combining covalent cross-links with non-covalent reversible hydrogen bond, and also with a full epoxy network, for comparison. Recovery of a 20 Joules impact damage was evaluated both through the analysis of impact curves, and visually, through an image analysis process. Progressive recovery was observed, up to 55 % with respect to the maximum impact force and 76 % regarding the dissipated energy after 24 h healing time at room temperature. This indicates that the healing ability of the matrix material is also effective when introduced in a 50 vol. % glass fibre reinforcement. Healing assessment through image analysis was performed over a longer healing period of 28 days, providing additional information on the kinetics of the self-healing process.

1 INTRODUCTION

Fibre Reinforced Composites (FRCs), due to their intrinsic heterogeneity, are generally affected by complex multi-scale failure mechanisms leading to the formation of matrix cracks that are difficult to detect and repair [1-5]. FRCs with the ability to heal and recover at least part of their initial properties after damage could present a solution to extend their lifetime and reliability. A possible approach is to introduce external healing agents in the matrix of the composite, through capsules or micro-channels, but this is often difficult to achieve when the matrix material is within a high fibre volume fraction composite [6-9]. An alternative approach is to rely on intrinsic self-healing polymers as matrices, which alleviates the need for additional phases beyond matrix and reinforcement. Several types of self-healing polymers are currently developed, some based on the use of thermoplastic/thermoset blends that repair through bonding of the thermoplastic phase at a certain temperature [10-13], some through the presence of reversible chemical bonds, through the presence of click reactions, or dynamic covalent bonds, that can reform by external trigger such as light or temperature, or at room temperature [14-16]. The present work investigated this last approach, by exploring the feasibility of processing glass fabric reinforced composites based on supramolecular hybrid network self-healing matrices and analysing their resulting properties and transfer of the self-healing ability to the composite. For this, composites were processed with the self-healing polymer Reverlink® HR-NR (HN-50-NC) from Arkema, combining covalent cross-links with non-covalent reversible hydrogen bonds [17-19] as the matrix, infused into glass fibre reinforcements.

In a previous publication [20], the feasibility of producing self-healing composites using the partially supramolecular self-healing polymer HN-50-NC and woven glass fabric through a simple and efficient "high temperature" VARIM process (at 150 °C) was demonstrated. This processing technique allowed fabricating glass-reinforced composites presenting a fibre volume fraction of 50 % and a reasonably low average porosity. Furthermore, dynamic thermo-mechanical measurements indicated that the resulting materials retain the very good damping properties of the matrix, with a damping ratio greater than 0.5 over a large temperature range. Self-healing properties were also evaluated by means

of bending tests showing a high recovery of around 65% of the maximum flexural strength, and of 72% of the bending stiffness after 24 h healing at room temperature.

The present work aims to investigate the applicability of these supramolecular matrix based fibre reinforced composites for impact protection. The method generally followed to investigate the self-healing ability of stiff FRCs after impact damage is through the analysis of residual compressive strength by means of Compression After Impact (CAI) tests [21-23]. In the present case, the flexibility of the matrix hindered the applicability of this technique [19, 20], therefore impact recovery was investigated both by evaluating the recovery of the maximum impact force and dissipated energy during impact, and "visually", by investigating damage restoration through image analysis.

2 MATERIALS AND METHODS

2.1 Materials

A commercially available partially supramolecular self-healing polymer, Reverlink® HR-NR (hereafter referred to as HN-50-NC) from Arkema, was selected as matrix material. It is composed of a blend of polycarboxylic fatty acids reacted with H-bonding heterocyclic primary amine (UDETA) and diepoxide (DGEBA). The curing cycle recommended by Arkema is 24 hours at 130 °C, as this system is not catalysed. After curing, the final polymeric network presents a combination of covalent bonds and supramolecular hydrogen-bonding crosslinks (50:50 %mol), the latter providing interesting self-healing ability to the cured material. A complete description of HN-50-NC synthesis and curing process, as well as a characterization of its thermo-mechanical properties, tensile properties and self-healing ability in function of self-healing time is provided in ref. [19].

In parallel, the commercial benchmark epoxy system Araldite LY 8615 + Aradur 8615 (100:50 in weight, from Huntsman) was selected for comparison. It is a high glass-transition temperature (T_g) epoxy resin, able to reach a T_g between 206 and 217 °C following a curing cycle of 90 min at 80 °C, followed by 60 min at 150 °C and a final post-curing of 60 min at 180 °C, according to the manufacturer's recommended cure schedule.

The glass fibre reinforcement was a woven twill 2x2 E-glass fabric, with a nominal areal weight of 390 g/m^2, 6 end/cm for warp fibres and 6.7 picks/cm for weft fibres, fibre diameter of 9 µm, yarn thickness of 0.45 mm, warp tex of 68x5 and weft tex of 272, from Suter-Kunststoffe AG.

2.2 FRCs processing and sample preparation

A modified Vacuum Assisted Resin Infusion Moulding (VARIM) was developed and used for processing glass fibre reinforced HN-50-NC based composites. Traditional VARIM process is performed at room temperature, using low viscosity resins (viscosity lower than 1 Pa·s is generally recommended as a first rule of thumb). In the present case, the starting prepolymer presented a too high viscosity at moderate temperature, measured to be around 385 Pa·s at 50 °C, it was therefore necessary to adapt the VARIM process to high temperatures.

Layers of fibre reinforcement were cut in 20x25 cm rectangles and stacked with a sequence of $[(+45/-45)/(0/90)]_{4s}$, aiming a final plate thickness of 5mm (corresponding fibre volume fraction (V_f) of 50%). The preforms to be infused were prepared following the lay-out as depicted in Figure 1 and all the consumables were chosen to withstand temperatures higher than 150 °C.

Preform preparation was carried out as follows: three layers of release agent were applied onto a teflon-coated aluminium plate. Glass fabric layers were stacked following the desired stacking sequence onto the plate. The whole stack was then covered with a peel ply and a distribution mesh (Infuplex OM70 PA, Diatex). The mesh was slightly shorter in length compared to the fabric layers in the infusion direction, so that the resin front slowed down and had sufficient time to fully impregnate the fabric before reaching the outlet. The inlet and outlet consisted of nylon 6,6 spirals (Airtech Europe Sarl) connected to silicon hoses and wrapped into expandable braided PET hoses, both provided by Suter-Kunstoffe AG, to homogeneously distribute the resin along the fabric layers' width. Finally, a flexible outer bag (Vacfilm400Y272, Cytec) was sealed with sealant tape (Tacky Tape® SM5142, Cytec) over the plate.

Since at 130 °C (curing temperature) the viscosity of the resin is still too high, a processing temperature of 150 °C was considered as an acceptable compromise, with about 20 min under 5 Pa·s viscosity [20]. Therefore, prior to infusion, both the matrix and the preform were pre-heated at 150 °C. In order to overcome pot-life limitations, the resin was divided in two different pots and heated and degassed (at 150 °C as well) at different moments of the infusion process, with around 30 minute gaps. Several preliminary infusions were performed in order to determine the best conditions for the infusion to take place. The whole infusion process was carried out at 150 °C and lasted about 1 hour (without considering resin pre-heating time) while the vacuum pressure difference was maintained at 1 bar.

Once infusion was completed, the temperature was decreased to 130 °C and the plate was let to cure for 22 hours. Samples were cut from the cured plates using a Maïco saw equipped with a diamond blade and then stored in a desiccator at room temperature (25 °C and 25% relative humidity) until testing.

Infusion of the epoxy system Araldite LY 8615 + Aradur 8615 was, instead, performed at room temperature, after a 30 min degassing step. Consequently, the recommended curing cycle was used, giving rise to a high T_g matrix.

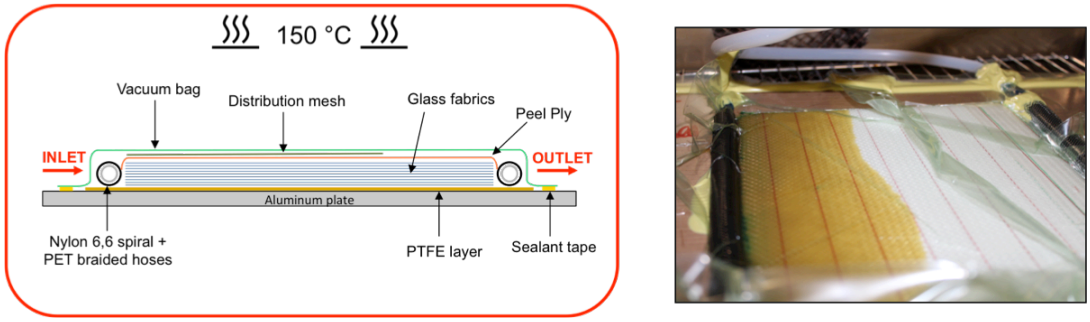

a) b)

Figure 1: Schematic representation of a VARIM set-up: preform (a) side view; (b) picture of a preform during infusion.

2.3 Impact test

In this work, impact test was carried out both to investigate the impact response of self-healing supramolecular based FRCs compared to traditional epoxy-based FRCs, as well as tool to study their self-healing ability.

Low velocity impact tests were performed using two different free fall impact towers:

- Instrumental Falling Weight Impact Tester (Rosand IFW): this impact tester has a 6 bar pressure circular clamping ring (70 mm diameter) with automated weight manipulation, an aluminium hemispherical impactor of 16 mm diameter and an impacting mass of 5.5 kg. Samples 10x10x0.5 cm were tested with this rig.
- Custom made free fall impact tower: this impact tower was built according to D7136 standard, it has an impactor mass of 5.5 kg, an hemispherical impactor tip of 16 mm diameter and a corner point clamping system. Samples 15x10x0.5 cm were tested with this rig.

Rosand IFW was used for the healing assessment through image analysis since the clamping system of the machine allowed obtaining larger areas of impact, while the custom made free fall impact tower was adopted to analyse impact curves, that could not have been obtained using the Rosand IFW.

In both cases, samples were impacted with 20 J energy, corresponding to a falling height of 0.37 m, mostly inducing delamination damage and little fibre damage.

Healing assessment by image analysis was performed taking advantage of the translucency of HN-50-NC composites and the fact that glass fibres in the composite transmit light in a virgin state, but

that when impacted and delaminated, opaque zones appear. After impact, samples were positioned close to a negatoscope and photographs were taken just after impact, and at increasing intervals (up to 28 days). Image treatment through Matlab software was then performed to quantitatively analyse damage area reduction over time.

In order to achieve this aim, first an active area (area of impact damage) was defined using the first and the last images via an edge detection algorithm in Matlab. Consequently, images were converted from **RGB** (Red-Green-Blue) space to **HSV** (Hue-Saturation-Value) space. Indeed, in the RGB domain, for tracking colour changes (from black at the damaged state to yellow in fully healed state, see Figure 6(a)), 3 parameters have to be considered at the same time and a one-to-one mapping cannot be obtained between the state of healing and RGB space. HSV space is a cylindrical space so it is again defined by three parameters: **Hue**, corresponding to the angle around the central vertical axis, **Saturation,** the radial distance from the centre of the cylinder and **Value** (or brightness or lightness), which is the distance along the axis. In our images, the saturation is almost constant for all images and for all pixels over time. Therefore, images are defined by a 2D space (**Hue** and **Value**). Furthermore, **Hue** values remains constant overtime for each pixel, so that changes in the images can be defined as a function of only one parameter, **Value**. Therefore, for each image and for each pixel the change of the **Value** parameter is tracked and it is defined to be linearly related to the healing progression of the sample, allowing to finally calculate the healing efficiency map η for each image in accordance with Equation 1, where Γ represents a general material property, in the present case the **Value** parameter.

$$\eta = \frac{\Gamma_{healed} - \Gamma_{unhealed}}{\Gamma_{virgin} - \Gamma_{unhealed}} \tag{1}$$

Healing efficiency is defined for each pixel to define a local healing map, the **Value** for the virgin case being chosen as an average value from an undamaged region, and the unhealed **Value** was chosen as the worst-case value of the pixel array at time 0. The average healing efficiency, for one sample as a function of time, is also evaluated with Equation 1, where the **Value** of healed region is the average of the healed values for each pixel in the Region of Interest, at a given time.

Another evaluation of healing performance was instead achieved through the analysis of impact curves. During impact, force versus time was recorded, as well as inbound and outbound velocities; dissipated energy (E_d) values were calculated as:

$$E_d = \frac{1}{2} m(v_{in} - v_{out})^2 \tag{2}$$

where m is the impacting mass and v_{in} and v_{out} the inbound and outbound velocities respectively.

In order to evaluate the self-healing efficiency, impacted samples were stored in a desiccator for 24h before being impacted again at the same location, and data were analysed in terms of maximum impact force values (F_{max}) and dissipated energy (E_d), as calculated from the inbound and outbound impactor velocities. Self-healing efficiency was calculated from the recovery of these parameters, using Equation 1 where "unhealed values" were obtained by a batch of samples that were re-impacted directly after the first impact event (0 h self-healing time). Three samples were tested per batch.

3 RESULTS AND DISCUSSION

Figure 2 compares typical load vs. time curves during impact of Araldite epoxy matrix (GF/Araldite) and HN-50-NC matrix (GF/HN-50-NC) composites.

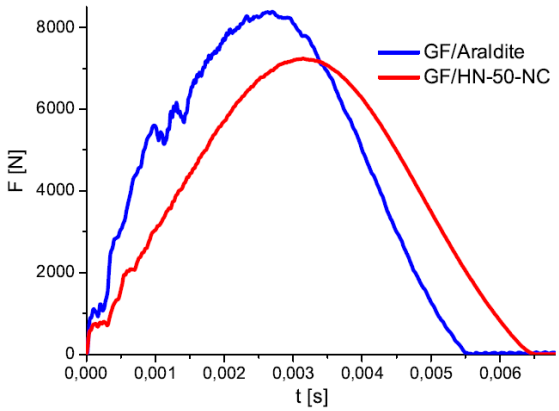

Figure 2: Example of Load vs. Time curves of Araldite epoxy matrix and HN-50-NC matrix composites impacted with 20J energy.

The initial knee found in the load-time plot is due to the inertia effect of the tup and the sample. The curve corresponding to the Araldite epoxy matrix composite has an asymmetric shape, presenting a rugged ascending segment and smoother descending one, typical for epoxy based laminates [24, 25]. The sharp drops in the load-time curve correspond to successive events of damage initiation and propagation; at a force around 5500 N the first of such events can be recognized.

On the other hand, HN-50-NC matrix composites display a smooth curve without discontinuities. Furthermore, they are characterised by a slightly lower peak impact force, by about 1000 N, and slightly larger contact duration. Both these parameters are attributed to the lower stiffness of these composites compared to epoxy-based ones (flexural moduli respectively of around 7 versus 14.7 GPa [20]). In addition, HN-50-NC matrix composites present a lower slope, which is designated as the contact stiffness. The higher strain ability of HN-50-NC matrix allows higher deformation of the sample during impact event without damaging the composite structure and making the impact head rebound with more force.

Dissipated energy was calculated from the inbound and outbound velocities of the impactor and resulting values are reported in Table 1. This energy corresponds to the amount of energy absorbed mainly in damage mechanisms but also in other non-conservative phenomena, such as vibrations, friction, specimen/fixture slipping, and that is not, therefore, restituted to the rebounding impactor [26]. In the present case, HN-50-NC composites dissipate 2 J more energy than Araldite epoxy ones, which indicates as expected a higher dissipation for the first composite, nonetheless dominated by the presence of glass fibres.

Figure 3 presents pictures of an Araldite epoxy and a HN-50-NC composite sample after being subjected to impact events. Important differences can be observed in the damaged area. In the Araldite epoxy sample, the damaged zone is small and concentrated around the impact point, where an indentation is present; damage propagates through the thickness with a cone shape as matrix and fibres start to break. No indentation is visible on HN-50-NC samples, where damage propagated to a greater extent in terms of diameter (mainly as intralayer delamination) but with a weaker global effect.

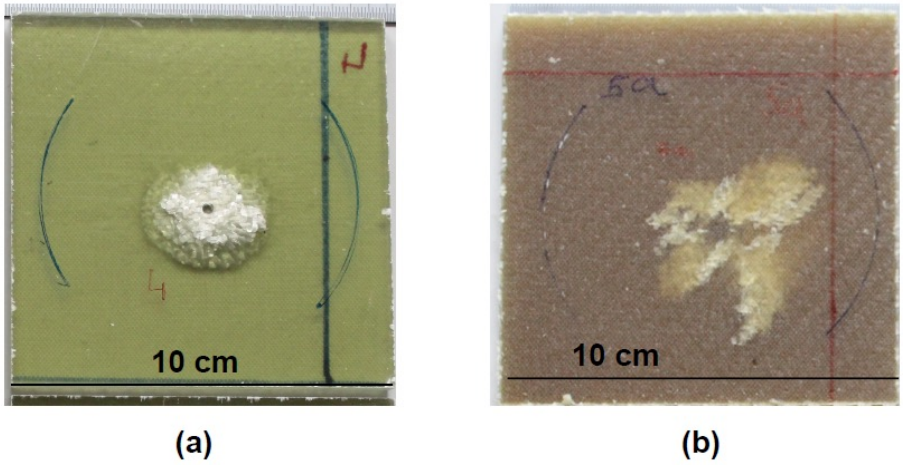

Figure 3: Images of (a) Araldite epoxy matrix and (b) HN-50-NC matrix composite sample after impact event.

To evaluate the ability of HN-50-NC to recover impact damage, impacted samples were stored for 24 h in a desiccator and consequently subjected to a new impact in the same location as the first and using the same impact energy. In order to define properties of un-healed samples, a batch of samples was subjected to a second impact right after the first one (0 h healing time).

Figure 4 shows examples of impact curves obtained after the first impact (virgin properties), at 0 h healing time (unhealed properties, indicated as second impact on the curve) and after 24 h healing time (healed properties). Table 1 reports average values of maximum impact load and dissipated energies.

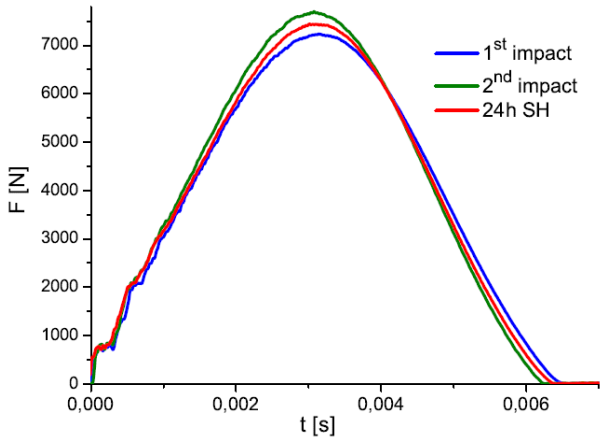

Figure 4: Example of Load vs. Time curves of HN-50-NC matrix composite samples after different impact events.

The first impact shows the lowest maximum load, while the second (0 h SH) gives the highest. Self-healed samples show maximum loads in between these first two. This behaviour is attributed to the presence of delamination damage in the impacted sample, leading to an overall loss in elasticity which makes the dissipated energy decrease, and ultimately the plate withstands a higher impact load. After 24 h healing time, intermediate values are observed due to the regain of some lost elasticity.

The same behaviour after first and second impact can be observed in Araldite epoxy matrix composites, as reported in Figure 5 that shows an example of two curves, one belonging to a sample that underwent one impact event and one belonging to a sample subjected to two consecutive impacts.

This graph shows, in addition to an increase of maximum peak load, that the sample subjected to two impact events presents a smooth curve. This is an indication that 20 J energy is not sufficient to initiate new damage in the impacted sample. Coherently, only 5 J of impact energy were dissipated during the second impact event. A slight decrease of dissipated energy at 0 h healing time is also observed for HN-50-NC based composites, which is partially recovered after 24 h healing (Table 1).

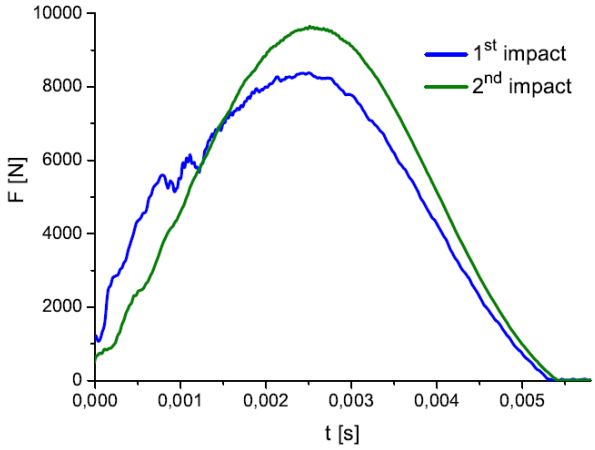

Figure 5: Examples of Load vs Time curves of Araldite epoxy composite samples after first and second impact events.

Healing efficiency of the composite samples was then calculated according to Equation 1, in terms of maximum force and dissipated energy recovery. The calculated healing efficiencies are reported in Table 1 together with average values of maximum impact force and dissipated energy of virgin, unhealed and healed samples.

Samples	Impact	Maximum Impact Force [N]	Dissipated Energy [J]
GF/HN-50-NC	1st Impact	7418±103	10.9±0.5
GF/HN-50-NC	2nd Impact (0h SH)	7606±134	10.0±0.1
GF/HN-50-NC	24 h Healing	7506±194	10.6±0.2
SH Efficiency η		55%	76%
GF/Araldite	1st Impact	8424±41	8.4±0.2
GF/Araldite	2nd Impact (0h SH)	9570±71	5.0±0.4

Table 1: Average maximum impact load, average dissipated energy values for GF/HN-50-NC and GF/Araldite composites and self-healing efficiencies obtained through impact test for GF/HN-50-NC composites.

Satisfactory recovery values can be observed, around 55 % with respect to the maximum impact force and 76 % regarding the dissipated energy. This value is in agreement with previous findings on the neat matrix [19]. However, differences among maximum impact forces and dissipated energy values of the different impact events are narrow, probably due to the low impact energy used to perform the test and, furthermore, standard deviation relative to these values are quite important. Hence, the self-healing values can be only taken here as indicative values.

Mechanical evaluation of healing ability towards impact damage was conducted in parallel with an assessment based on image processing. This was possible thanks to the translucent properties of HN-50-NC and the fact that glass fibres in the composite transmit light in a virgin state, but that when impacted and delaminated, opaque zones appear. Therefore, through strong backlighting, the damaged area was clearly visible (Figure 6(a), 0h) and the resorption of impact damage was followed taking pictures at regular time intervals for around 28 days.

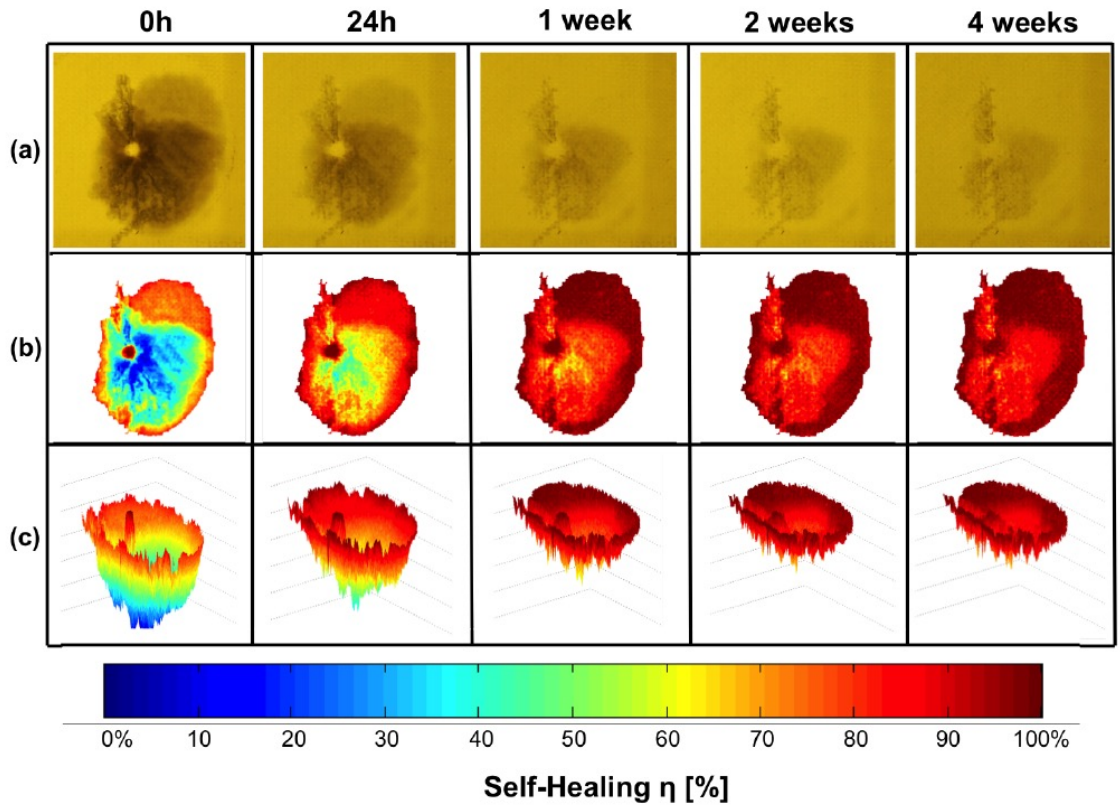

Figure 6: (a) Pictures of recovery of impact damage, (b) 2D and (c) 3D damaged zone healing maps after different self-healing times (24h, 1, 2 and 4 weeks).

All images were then processed as described in Section 2.2 and healing efficiency maps were calculated as a function of healing time. The first row of pictures, denoted as (a), of Figure 6 illustrates the case of a sample that underwent a 20 J impact event, just after impact and after 4 different self-healing times (24h, 1, 2 and 4 weeks). A delaminated area of about 35 mm in diameter is observed just after impact, resulting from the optical contrast creating darker zones when cracks are present in the material. The following pictures clearly show a progressive recovery of the damage with time, until an almost complete restoration of the sample after 4 weeks of self-healing.

The evolution of healing profiles across the sample surface was also investigated. Figure 6 (b) and (c) report 2D and 3D maps of the local healing achieved in the damaged area over 4 weeks healing time. The extent of damage decreases in a radial fashion from the impact point over time. Furthermore, the greater the damage, the higher the rate of recovery. In addition, these graphs also point out the fundamental role of the first 24 h of recovery, reaching already 50 % of the total recovery achieved after 4 weeks over the whole sample.

Quantitatively evaluating this recovery by image analysis, Figure 7 reports the values of average self-healing efficiency as a function of self-healing time. In this special case, samples were not kept in a desiccator during the healing period. From this graph, information of the healing process and kinetics can be extrapolated.

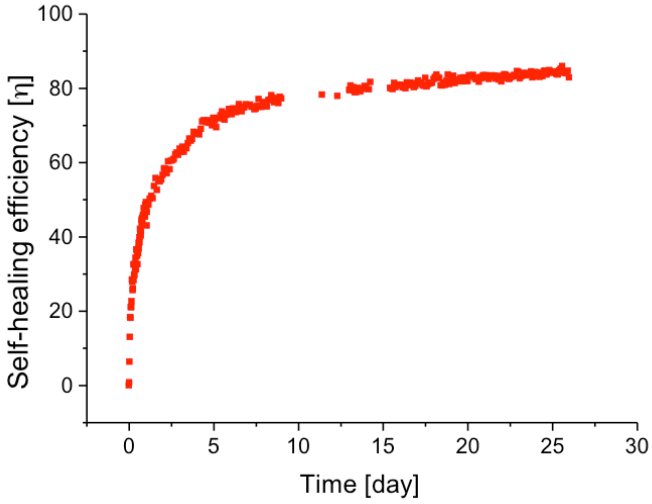

Figure 7: Self-healing efficiency vs. time as extracted from image analysis.

As for the neat polymer [19], the kinetics of healing is very fast for short healing times, reaching around 40 % average healing efficiency after the first day and around 50 % after 2 days, and then progressively slows down reaching slowly 80 % healing after 26 days. In this case, healing does not seem to reach 100%. This is attributed to partial fibre breakage leading to permanent change in transparency of the sample, and preventing the crack faces to get back in contact. As the samples were left to heal with no applied pressure to close cracks, healing took place, as described according to Figure 6, from the crack tip, progressively back to the centre of the impact zone. Nonetheless, even if it was not possible to quantify the recovery of mechanical properties of the plates, it is clear from this study that cracks tend to close back over time in these samples, leading to a restoration of the materials integrity.

4 CONCLUSIONS

In this work the damping properties and the ability to recover impact damage of glass fibre-reinforced composites based on a partially supramolecular self-healing matrix were investigated and compared to traditional epoxy-based FRCs. Supramolecular based FRCs were processed through a "high temperature" Vacuum Assisted Resin Infusion Molding (VARIM) obtaining good quality final materials. They were then subjected to 20 J impact events. Supramolecular based FRCs showed higher energy absorption compared to epoxy based materials, confirming our previous results [20].

The possibility of transferring the self-healing properties typical of the polymer matrix to the glass fibre reinforced composites was demonstrated: self-healing efficiency was evaluated both mechanically investigating the impact curves (over 24 h healing time), and visually, evaluating the progressive damage area reduction over time (28 days) through image analysis.

Impact tests revealed a recovery of respectively 55 % and 76 % of maximum impact force and dissipated energy respectively, after 24h. In agreement with what observed for the neat polymers, faster healing kinetics were observed at the beginning of the healing process, that progressively slowed down for longer healing times.

The composites processing route proposed here is compatible with further larger scale industrial interest, both in terms of materials and processing expenses. Furthermore, bending [20] and impact results lead us to envisage potential applications of the self-healing supramolecular based FRCs in impact protection or in the continuous damage recovery in flexural bending modes of flexible composite structures.

ACKNOWLEDGEMENTS

Funding from the European Union Seventh Framework Program [FP7/2007-2013] under grant agreement no. 290308 (Marie Curie ITN SHeMat `Self-Healing Materials: from Concepts to Market') is gratefully acknowledged. Arkema is thanked for kindly providing Reverlink HR-NR and for fruitful discussions, Huntsman Advanced Materials for providing the Araldite resin, and the LMAF for use of their impact testing equipment.

REFERENCES

[1] K. L. Riefsnider, K. Schulte, and J. C. Duke, Long term failure behavior of composite materials, *ASTM Special Technical Publications,* **813**, 1983, pp. 136-159 (doi: 10.1520/STP31820S).

[2] R. Talreja, Damage development in composites: Mechanisms and modelling, *The Journal of Strain Analysis for Engineering Design,* **24**, 1989, pp. 215-222 (doi: 10.1243/03093247V244215).

[3] R. Talrega, Damage Mechanics of Composite Materials, Vol. 9, Elsevier, New York, 1994.

[4] J.A. Nairn, *Matrix microcracking in composites*, Comprehensive Composite Materials, Vol. 2(13), Elsevier, New York, 2000.

[5] E.K. Gamstedt and R. Talreja, Fatigue damage mechanisms in unidirectional carbonfibre-reinforced plastics, *Journal of Materials Science,* **34**(11), 1999, pp. 2535-2546 (doi: 10.1023/A:1004684228765).

[6] S.R. White, N.R. Sottos, P.H. Geubelle, J.S. Moore, M.R. Kessler, S.R. Sriram, E.N. Brown and S. Viswanathan, Autonomic Healing of polymer composites, *Nature,* **409**, 2001, pp. 794-797 (doi: 10.1038/35057232).

[7] A.J. Patel, N.R. Sottos, E.D. Wetzel and S.R. White, Autonomic healing of low-velocity impact damage in fibre-reinforced composites, *Composites Part A: Applied Science and Manufacturing,* **41**(3), 2010, pp. 360-368 (doi: 10.1016/j.compositesa.2009.11.002).

[8] C.J. Norris, G.J. Meadway, M.J. O'Sullivan, I.P. Bond and R.S. Trask, Self-healing fibre reinforced composites via a bioinspired vasculature, *Advanced Functional Materials,* **21**(19), 2011, pp. 3624-3633 (doi: 10.1002/adfm.201101100).

[9] J.F. Patrick, K.R. Hart, B.P. Krull, C.E. Diesendruck, J.S. Moore, S.R. White and N.R. Sottos, Continuous self-healing life cycle in vascularized structural composites, *Advanced Functional Material,* **26**(25), 2014, pp. 4302-4308 (doi: 10.1002/adma.201400248).

[10] K. Pingkarawat, T. Bhat, D.A. Craze, C.H. Wang, R.J. Varley and A.P. Mouritz, Healing of carbon fibre–epoxy composites using thermoplastic additives, *Polymer Chemistry,* **4**(18), 2013, pp. 5007-5015 (doi: 10.1039/C3PY00459G).

[11] K. Pingkarawat, C. Dell'Olio, R.J. Varley and A.P. Mouritz, Poly(ethylene-co-methacrylic acid) (EMAA) as an efficient healing agent for high performance epoxy networks using diglycidyl ether of bisphenol A (DGEBA), *Polymer,* **92**, 2016, pp. 153-163 (doi: 10.1016/j.polymer.2016.03.054).

[12] A. Cohades, E. Manfredi, C.J.G. Plummer and V. Michaud, Thermal Mending in phase-separated Epoxy -polycaprolactone blends, *European Polymer Journal,* **81**, 2016, pp. 114-128 (doi: 10.1016/j.polymer.2016.03.054).

[13] A. Cohades and V. Michaud, Thermal mending in E-glass reinforced Poly(ε-caprolactone)/epoxy blends, *Composites Part A: Applied Science and Manufacturing,* 2017, *in print*.

[14] S.D. Bergman and F. Wudl, Mendable polymers, *Journal of Materials Chemistry,* **18**, 2008, pp. 41-62 (doi: 10.1039/B713953P).

[15] W.H. Binder, Self-Healing Polymers: from Principles to Applications, Wiley, New York, 2013.

[16] S. Garcia and H. Fischer, *Self-healing polymer systems: properties, synthesis and applications,* Smart Polymers and Their Applications, Woodhead Publishing, 2014, pp. 271-298 (doi: 10.1016/B978-0-85709-695-1.50017-0).

[17] D. Montarnal, F. Tournilhac, M. Hidalgo and L. Leibler, Epoxy-based networks combining chemical and supramolecular hydrogen-bonding crosslinks, *Journal of Polymer Science Part A: Polymer Chemistry,* **48**(5), 2010, pp. 1133–1141 (doi: 10.1002/pola.23870).

[18] Arkema: 'Reverlink Supramolecular Technology' http://arkema.com/.

[19] F. Sordo, S.J. Mougnier, N. Loureiro, F. Tournilhac and V. Michaud, Design of Self-Healing Supramolecular Rubbers with a Tunable Number of Chemical Cross-Links, *Macromolecules,* **48**, 2015, pp. 4394-4402 (doi: 10.1021/acs.macromol.5b00747).

[20] F. Sordo and V. Michaud, Processing and damage recovery of intrinsic self-healing glass fibre reinforced composites, *Smart Materials and Structures,* **25**, 2016, (doi: 10.1088/0964-1726/25/8/084012).

[21] H.R. Williams, R.S. Trask, and I.P. Bond, Self-healing composite sandwich structures, *Smart Materials and Structures,* **16**(4), 2007, pp. 1198-1207 (doi: 10.1088/0964-1726/16/4/031).

[22] T. Yin, M.Z. Rong, J Wu, H. Chen, and M.Q. Zhang, Healing of impact damage in woven glass fabric reinforced epoxy composites, *Composites Part A: Applied Science and Manufacturing,* **39**(9), 2008, pp. 1479 -1487 (doi: 10.1016/j.compositesa.2008.05.010).

[23] A.J. Patel, N.R. Sottos, E.D.Wetzel, and S.R. White, Autonomic healing of low-velocity impact damage in fibre-reinforced composites, *Composites Part A: Applied Science and Manufacturing,* **41**(3), 2010, pp. 360-368 (doi: 10.1016/j.compositesa.2009.11.002).

[24] G. Belingardi and R. Vadori, Low velocity impact tests of laminate glass-fibre-epoxy matrix composite material plates, *International Journal of Impact Engineering,* **27**(2), 2002, pp. 213-229 (doi: 10.1016/S0734-743X(01)00040-9).

[25] G.S. Chandekar, B.S. Thatte, and A.D. Kelkar, On the behavior of fibreglass epoxy composites under low velocity impact loading, *Advances in Mechanical Engineering,* **2**, 2010, (doi: 10.1155/2010/621406).

[26] P. Feraboli and K.T. Kedward, Enhanced evaluation of the low-velocity impact response of composite plates, *AIAA Journal,* **42**(10), 2004, pp. 2143-2152 (doi: 10.2514/1.4534).